EPJ Web of Conferences **158**, 01003 (2017) DOI: 10.1051/epjconf/201715801003
QFTHEP 2017

Nucleus-nucleus interactions in very-high-energy cosmic ray experiments

Anatoly Petrukhin* and *Aleksei* Bogdanov
National Research Nuclear University MEPhI (Moscow Engineering Physics Institute),
115409, Russian Federation, Moscow, Kashirskoe shosse, 31

Abstract. A review of unusual results of experiments in cosmic rays which cannot be explained in the frame of the existing models of hadron interactions is presented. Requirements to features of a new model which are necessary for explanation of all observed unusual events and phenomena are formulated. A model of hadron interactions with production of QGM blobs with large orbital momentum is considered. Its possibilities for explanation of various unusual events and phenomena are discussed.

1 Introduction

In collider physics, overwhelming majority of investigations (both experimental and theoretical) are connected with proton-proton interactions. It is clear that these interactions are more simple as for experimental analysis so for theoretical description then nucleus-nucleus interactions. In the last case various types of collective interactions of nucleons or quarks and gluons may appear.

In cosmic rays it is impossible to investigate proton-proton interactions since targets in the Earth's atmosphere are the nuclei of nitrogen and oxygen atoms. Additionally, most parts (about 60%) of cosmic rays are nuclei of various elements (up to iron) which come from cosmic space.

Above the energy of about 10 GeV primary cosmic ray (PCR) energy spectrum is described by a simple formula $dN/dE \sim E^{-\gamma}$, where $\gamma \approx \text{const} \approx 2.7$. In cosmic ray investigations, particles with energies up to about 10^{20} eV and some features in the behavior of the energy spectrum were observed. Possible classification of CR energy intervals is given in Table 1. Energy in the center-of-mass system (CMS) is usually calculated for nucleon-nucleon system $\sqrt{s_{NN}}$ irrespective of the type of interactions: nucleon-nucleon, nucleon-nucleus, nucleus-nucleus.

Composition of cosmic rays, or more exactly the relation between different components of cosmic rays, depends on the energy taken into account: energy per nucleon or energy per nucleus. Relation between various components combined in several groups is given in the Table 2.

* Corresponding author: AAPetrukhin@mephi.ru

Usually, the value <ln A> is used as a parameter of composition. For normal composition, this value is equal to ≈ 1.5. In simulations very often limiting assumptions on the composition are used: pure protons (ln A = 0) and pure iron (ln A = 4).

Table 1. Classification of CR energy intervals.

CR energy, eV	Term	Energy in CMS, TeV	Main feature
$< 10^{15}$	High	< 1.4	–
$10^{15} – 10^{17}$	Very High	1.4 – 14	the knee
$10^{17} – 10^{19}$	Ultra High	14 – 140	the ankle
$> 10^{19}$	Extremely High	> 140	GZK cutoff

Table 2. Relation between various nucleus.

Particles	Z	<A>	Energy per nucleon	Energy per nucleus
Protons	1	1	92%	42%
α-particles	2	4	7%	21%
Light nuclei	3-5	10	0.25%	1%
Medium nuclei	6-10	15	0.5%	18%
Heavy nuclei	≥ 11	32	0.25%	18%

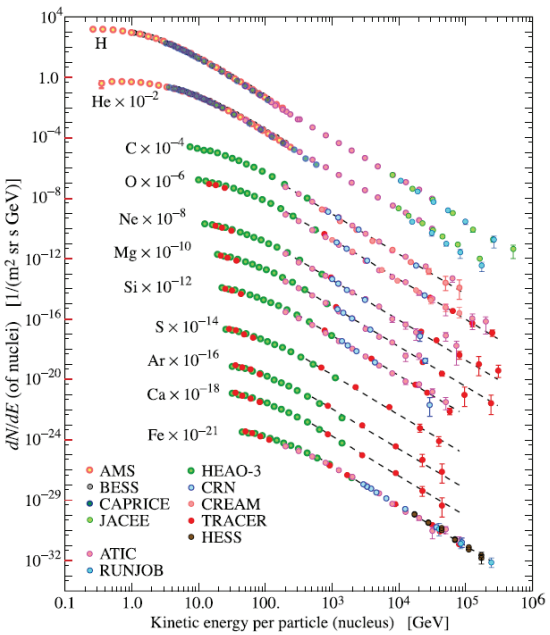

Fig. 1. Differential energy spectra of various cosmic ray nuclei obtained in direct measurements [1].

Investigations of cosmic rays are performed in space, at higher layers of the atmosphere, on the mountains, on the Earth's surface (near sea level), underground (under water and under ice). Outside of the Earth's atmosphere, direct measurements of primary particles (Z and E) by means of satellites are carried out. Taking into account a sharp decrease of CR flux with energy, such investigations can be carried out for energies less than 10^{15} eV only (Fig. 1). In the Earth's atmosphere, probability to detect primary particles is decreased very rapidly with increasing the depth.

Therefore on the ground level secondary particles can be investigated only. The most important phenomena generated by PCRs in the atmosphere are extensive air showers (EAS) which consist of various particles: hadrons, electrons, positrons, photons, muons and neutrinos, and they can reach the sea level starting from the energy near 10^{15} eV. EAS investigations are the only way to study CR energy region above 10^{15} eV.

For EAS investigations, systems of various detectors distributed over large area are applied. In addition to detectors of charged particles (mainly scintillation counters), detectors of different type radiations which are generated by EAS (Cherenkov light, fluorescence, radio, etc) are used.

The scheme of cosmic ray investigations by means of EAS observables is given in Fig. 2 [2].

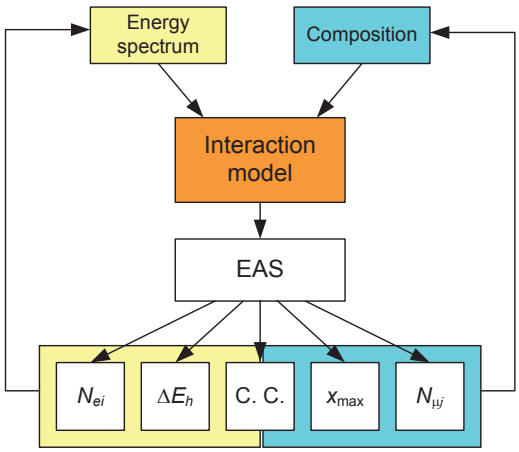

Fig. 2. Existing approach to EAS analysis.

Measured characteristics of EAS are: number of charged particles in each detector (N_{ei}), number of muons in each muon detector ($N_{\mu j}$), energy deposit of EAS core (ΔE_h), cascade curve (C.C., longitudinal profile of EAS development in the atmosphere) and maximum EAS development (X_{max}).

These experimental values are used for recalculation to primary energy spectrum and composition taking into account the interaction models which were checked at accelerator energies.

2 Results of cosmic ray experiments

Numerous experiments with various components of cosmic rays at primary particle energies below 10^{15} eV gave no deviations from a simple picture of CR energy spectrum (Fig. 1) and mass composition (Table 2). Though the results of several experiments showed

unusual behavior of some components (especially muons), they gave no serious deviations from an assumed picture.

Above 10^{15} eV the picture is changed drastically. The first unusual phenomenon was observed in 1957 [3]. It was so-called "the break" in spectrum of charged particle number at energy about 3 PeV, later named "the knee". There can be two reasons of its origin: cosmophysical (changes in the energy spectrum and/or the composition of PCR, and nuclear physical (changes in the interaction model). After first discussions, most part of physicists agreed with the first possibility taking into account that it is in a good agreement with the Galactic model of cosmic ray origin.

At the further advancement to higher energies, other phenomena were observed: the second knee, the ankle, etc. All these changes in EAS characteristics were explained by changes in PCR energy spectrum and composition, results are shown in Fig. 3 and Fig. 4.

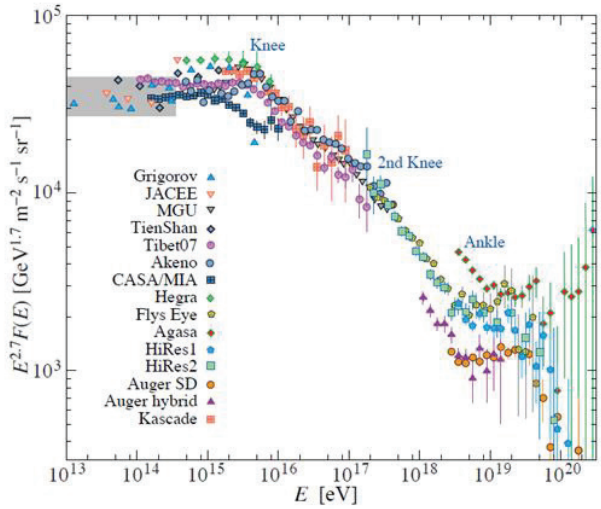

Fig. 3. All-particle energy spectrum of primary cosmic rays [1].

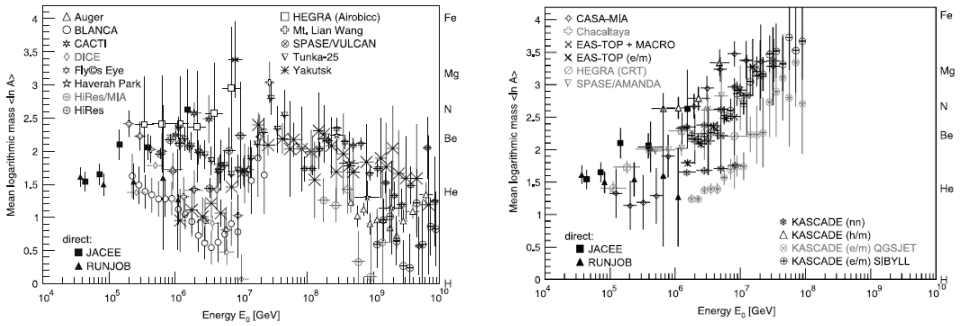

Fig. 4. Mean logarithmic mass of cosmic rays derived from the depth of the shower maximum (left), from the measurements of electrons, muons, and hadrons at ground level (right) [4].

Next serious deviations from the accepted picture of cosmic ray origin and existing model of their interactions were so-called unusual events which were detected at PeV energies and above in various experiments [5-7]. The list of such unusual events and phenomena includes:

- alignment (detection of three or more cascades which are located in a practically straight line; the probability of occasional generation of such events is negligibly small) – see Fig. 5;

- penetrating cascades (these cascades exhibit unusually slow absorption and correspondingly abnormally large attenuation length in comparison with the normal hadron cascade curve) – see Fig. 6;

- Centauros (observation of families with several tens of hadron cascades and practically without electromagnetic cascades) and Anti-Centauros (with opposite situation); these phenomena give evidence for the violation of isotopic invariance in secondary particle production;

- long-flying particles (these particles can penetrate a large thickness of matter and interact with the production of cascades);

- very young and very old EAS (with anomalous values of shower age), etc.

Possible reasons of their appearance were discussed in many papers, and various ideas of their explanation were proposed, see e.g. [8-12]. But no idea for their explanation from a single point of view was proposed.

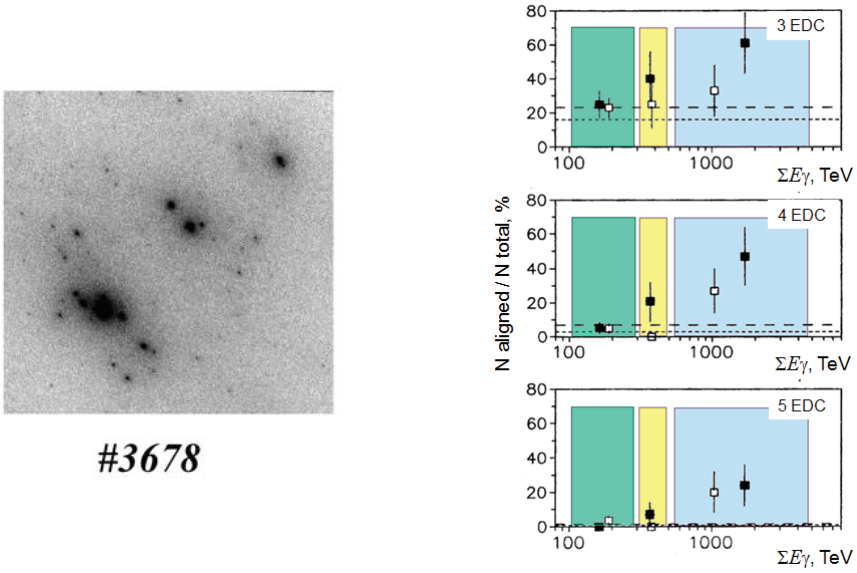

Fig. 5. Example of aligned event detected in Pamir experiment (left). Dependence of the fraction of families with alignment versus total γ-quanta energy of the event (right) [5].

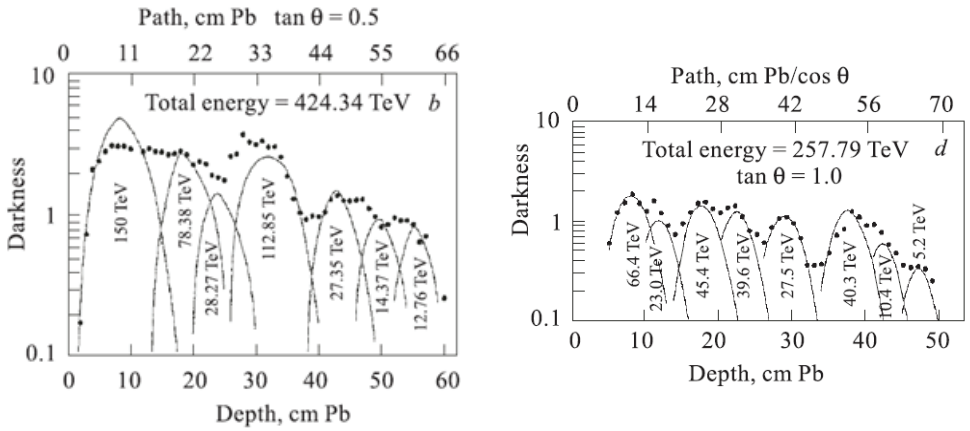

Fig. 6. Examples of events with penetrating cascades. Shower transition curve in spot darkness is shown [6].

3 Cosmic ray "muon puzzle"

During the last about 10 years, a new problem in cosmic ray muon investigations appeared. In several experiments, excess of muon bundles compared to simulations was observed. Firstly this excess was observed in LEP detectors ALEPH and DELPHI at muon multiplicity about 100 particles [13,14] (Fig. 7).

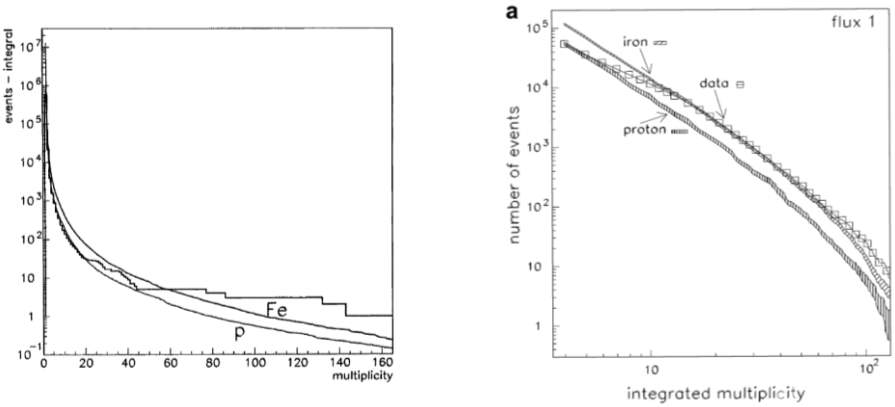

Fig. 7. Integral multiplicity distributions of muons in the TPC of ALEPH detector (left) [13] and in HAB of DELPHI detector (right) [14] compared to CORSIKA simulations for p and Fe.

However in these experiments there was no possibility to study the dependence of this excess on primary particle energies. This information was obtained in experiment NEVOD-DECOR in which muon bundles were measured at various zenith angles (Fig. 8 [15]).

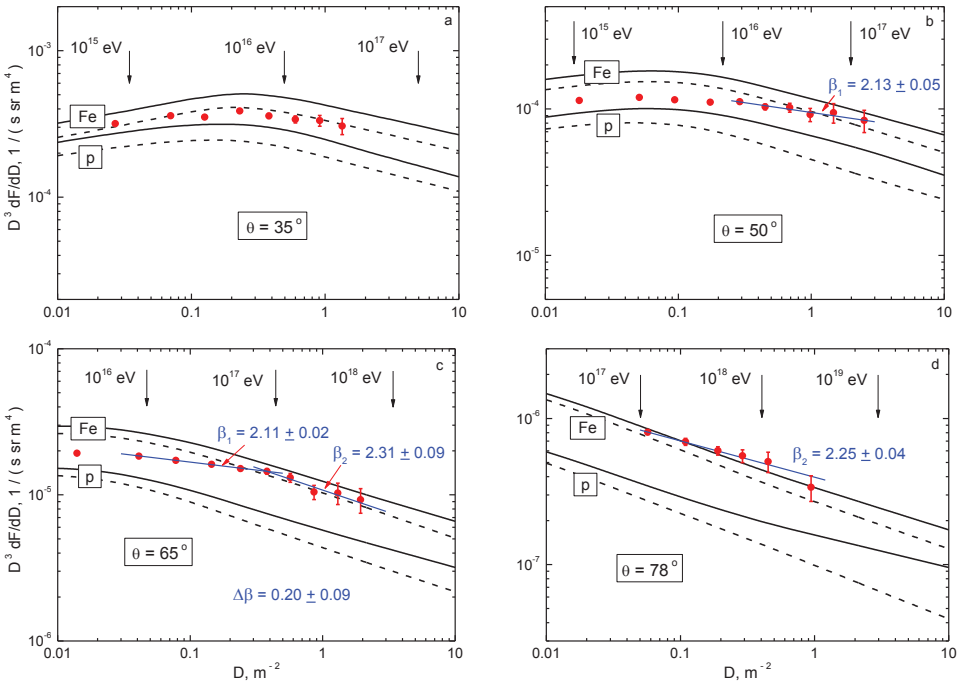

Fig. 8. Measured (points) and calculated (curves) differential local muon density spectra for 4 zenith angles [15].

For each zenith angle registered multiplicity m was re-calculated into local muon density (ratio of the number of muons that hit the setup to the detector area) and corresponding spectra were obtained, which are compared with results of simulations (Fig. 8). From Fig. 8a it is seen that at small zenith angles (35°) the experimental points are in a good agreement with calculations for normal energy spectrum and composition of cosmic rays, and even the knee in the interval 1-10 PeV is noticeable. Data for 50 and 65° (Fig. 8b,c) demonstrate a trend to a heavier composition and a hint for an increase of the slope near 10^{17} eV. However, at very high energies of primary particles around 10^{18} eV and above, which correspond to the last interval of zenith angles (78°, Fig. 8d), intensity of muon bundles is higher than predictions even for pure iron primary flux.

This result was confirmed in Auger experiment [16], where the number of muons exceeds the expected values for pure iron composition, too, and the excess increases with increasing energy of primary particles (Fig. 9). At the same time HiRes [17] and Auger [18] data on X_{max} distribution favor a light (predominantly proton) primary composition near 10^{18} eV.

The last measurements of muon energy spectrum above 100 TeV [19] also showed serious deviations from usual energy spectrum (Fig. 10).

The set of the listed results on the study of both the muon component of the EAS and single muons of cosmic rays is the so-called “muon puzzle” [20]. Obviously, in the frame of existing models of cosmic ray origin and their interaction it is impossible to find a solution of this muon puzzle, and introduction of a new model of interaction is required.

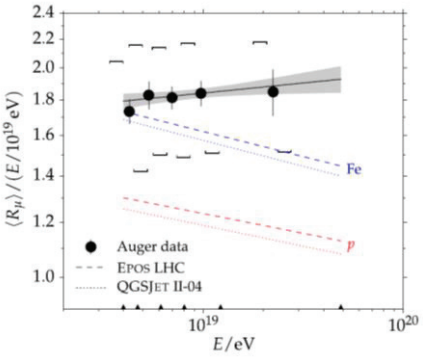

Fig. 9. Average muon content as a function of the shower energy [16]; shown for comparison are theoretical curves for proton and iron showers.

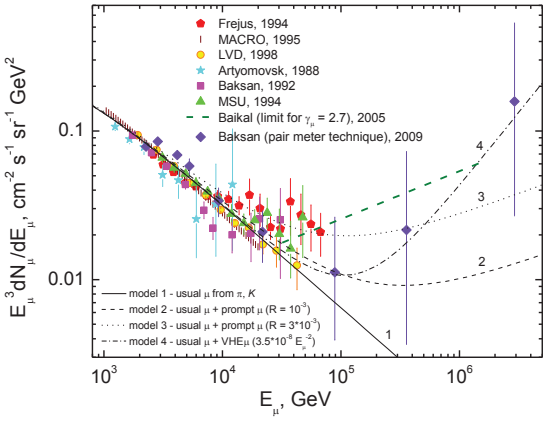

Fig. 10. Differential muon energy spectra for vertical direction measured in various experiments; the curves correspond to different spectrum models [19].

4 A new model of nucleus-nucleus interactions

What we need for explanation of all unusual data from a single point of view? A model of hadron interactions is required which gives:

1) threshold behavior (unusual events appear at several PeV only);
2) large cross section (to observe unusual events in CR);
3) large orbital momentum (to explain alignment);
4) large yield of HE leptons (excess of muon bundles, penetrating cascades);
5) the change of EAS development and, as a consequence, increasing N_μ/N_e ratio.

Which kind of model can be acceptable for this? The first, production of new heavy particles. But in this case the geometrical cross section will be very small

$$\sigma \sim \pi \lambda\!\!\!^{-2}, \quad \lambda\!\!\!^{-} \sim 1/m \tag{1}$$

The second, production of blobs of quark-gluon plasma (QGP), though it is better to speak about quark-gluon matter (QGM), since usual plasma is a gas, while quark-gluon plasma behaves like a liquid. We will consider the last model, since it allows explain the inclusion of new interaction features observed in LHC and cosmic ray experiments.

Production of QGM blobs provides two main conditions:

- threshold behavior, since for that high temperature (energy) is required;
- large cross section, since the transition from quark-quark interaction to some collective interaction of many quarks and gluons occurs:

$$\sigma \sim \pi \lambda\!\!\!^{-2} \to \sigma \sim \pi R^2 \tag{2}$$

where R is the size of quark-gluon blob.

But for explanation of other observed phenomena, a large value of orbital angular momentum is required. The question about orbital momentum which must appear in nucleus-nucleus interactions is usually not considered. For example in Fig. 11 the pictures from [21,22] are presented.

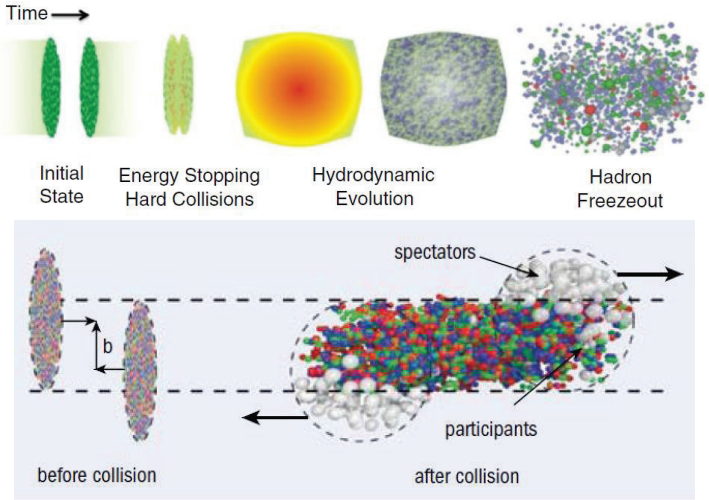

Fig. 11. The time evolution of a high-energy heavy-ion collision (top) [21]. Participants and spectators at the heavy-ion fireball (bottom) [22].

As one can see from this figure, QGM which is produced in peripheral collision, has no orbital momentum. Firstly, the importance of orbital momentum in heavy ion collisions was discussed in paper [23]. Corresponding scheme is presented in Fig. 12. Further investigations of the value of orbital momentum L were done in [24]. It was shown that the value of the orbital momentum for gold-gold collisions with energy 200A GeV (about 40

TeV) can reach $L \sim 10^4$. A blob of a globally polarized QGM with a large orbital angular momentum can be considered as a usual resonance with a large centrifugal barrier. The centrifugal barrier

$$V(L) = L^2/2mR^2 \tag{3}$$

will be large for light quarks but much less for top-quarks or other heavy particles. Though in interacting nuclei top-quarks are absent, the suppression of decays into light quarks gives time for the appearance of heavy quarks in boiling quark-gluon matter in the blob.

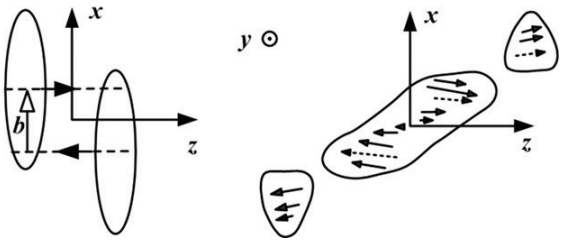

Fig. 12. Production of orbital angular momentum in non-central ion-ion collisions [22].

Simultaneous interactions of many quarks change the energy in the center of mass system drastically:

$$\sqrt{s} = \sqrt{2m_p E_1} \to \sqrt{2m_c E_1}\,, \tag{4}$$

where $m_c \approx nm_N$. At threshold energy, $n \approx 4$ (α-particle).

Produced $t\bar{t}$ -quarks take away from the QGM blob the energy $\varepsilon_t > 2m_t \approx 350$ GeV, and taking into account fly-out energy $\varepsilon_t > 4m_t \approx 700$ GeV in the center of mass system.

Top-quarks decay $t(\bar{t}) \to W^+(W^-) + b(\bar{b})$, W-bosons decay into leptons (~ 30%) and hadrons (~ 70%), b-quarks produce jets which generate multiple pions decaying into muons and neutrinos.

5 Explanation of CR and LHC results

In cosmic rays the new model allows explain all observed phenomena [25], in the fist turn "muon puzzle". Decays of W-bosons into muons and neutrinos explain excess of VHE muons with energy above 100 TeV (Fig. 13) and appearance of penetrating cascades [26]. Decays of W-bosons into hadrons (mainly pions, in average ~ 20) explain the increasing muon number (muon excess) with increasing energy.

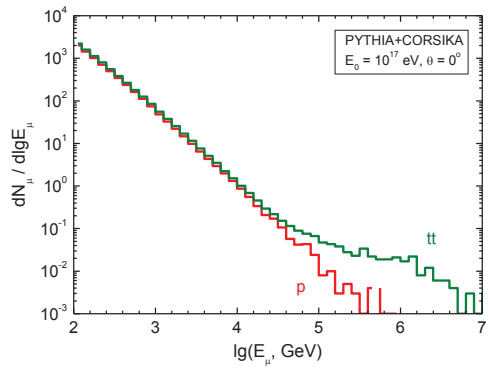

Fig. 13. The inclusive muon energy spectrum simulated by means of the CORSIKA code taking into account t-quarks pair production according to PYTHYA.

Let us consider the influence of the new model on interpretation of results of EAS investigations. Now the transition from measured data to the EAS energy does not take into account a missing energy which is carried away by VHE muons and three types neutrinos, and a change of EAS development due to a change of interaction model. A sharp increase of the missing energy leads to a change of EAS energy spectrum if this effect is not taken into account at reconstruction of EAS parameters from experimental data (Fig. 14).

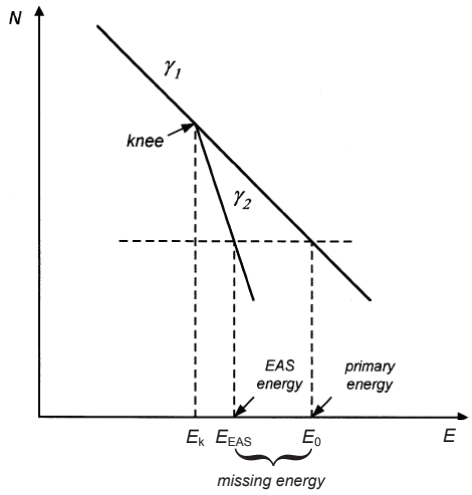

Fig. 14. Influence of missing energy on CR energy spectrum behavior.

A similar situation is connected with the change of the measured composition of CR. The threshold value of $\sqrt{s_{AA}}$ for iron nuclei will be attained at lower energy than for lighter nuclei. Therefore the number of registered EAS from iron and other heavy nuclei will be increased compared to EAS from more light nuclei (Fig. 15). If not to take into account the change of interaction model at transition to PCR energy spectrum and mass composition, this will lead to overestimation of heavy nuclei fraction in PCR.

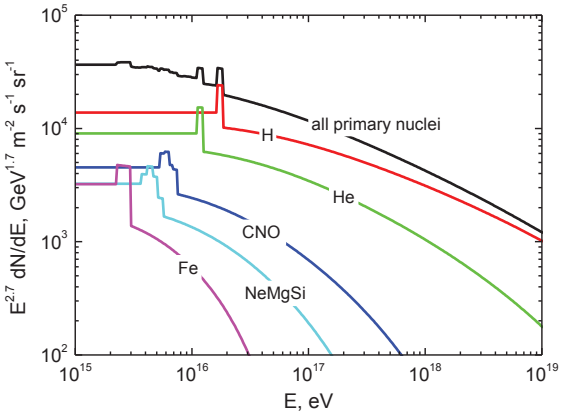

Fig. 15. Changes of various CR nuclei spectra in the frame of the considered interaction model.

The detailed discussion of explanation of other unusual events observed in CR experiments can be found in [27,28].

To illustrate possibilities of the new model for explanation of unusual phenomena observed in nucleus-nucleus collisions at LHC, let's consider two examples.

The first example is observation of imbalance of jet energies at ATLAS in heavy ion collisions (Fig. 16) [29].

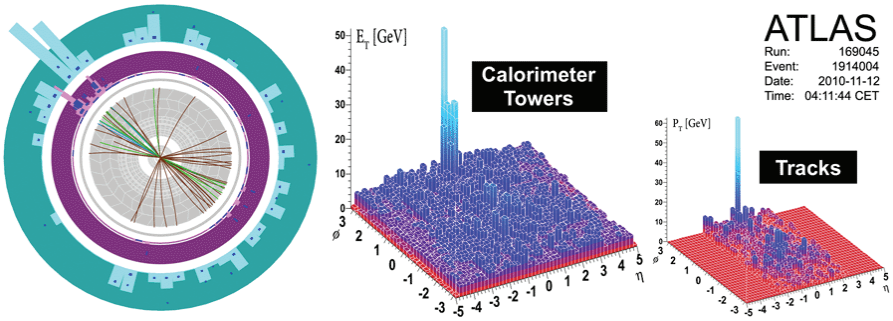

Fig. 16. Highly asymmetric dijet event in the ATLAS detector at Pb-Pb collision [29].

If to take into account a possibility of $t\bar{t}$ -quarks pair production, explanation will be the following: top-quark decays as $t \to W + b$, and kinetic energy of particles in the center-of-mass system will be equal to: $T_b \approx 65$ GeV, $T_W \approx 25$ GeV. If to take into account the fly-out energy, T_b may be more than 100 GeV which corresponds to jet energy in the observed event. In a case of decay W into pions (more than 10 particles), a picture observed by ATLAS will be obtained.

The second example is an excess of secondary particles observed in nucleus-nucleus (Pb-Pb) collisions compared to proton-proton collision at the same energy in the center-of-mass system $\sqrt{s_{NN}} \approx 2.76$ TeV [30]. If to take into account collective interactions, the average mass of intersecting parts of nuclei will be larger than nucleon mass, and corresponding value $\sqrt{s_{AA}}$ will be larger, too. Therefore, experimental point at the diagram must be moved to the right (Fig. 17).

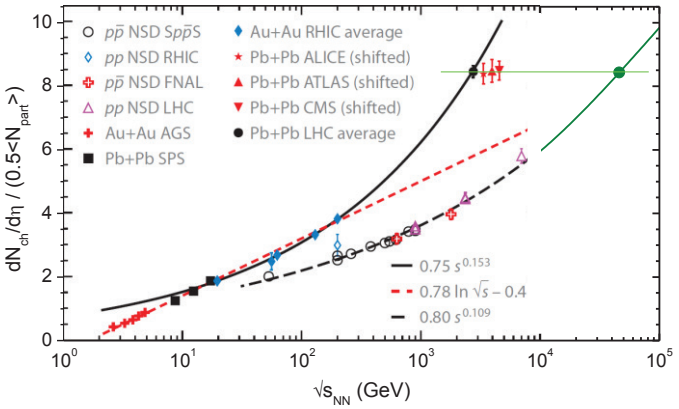

Fig. 17. Multiplicities of charged particles formed in nucleus–nucleus and proton–proton collisions as a function of collision energy [30].

If to take into account that $\sqrt{s_{AA}}$ cannot be less than $\sqrt{s_{NN}}$, it allows evaluate limiting average number of interacting nucleus (see Fig. 17): $\sqrt{n_N}$ < 50 TeV / 3.5 TeV ≈ 14. So in Pb-Pb interactions a blob of QGM can consist of up to 200 nucleons.

6 Conclusion

The results obtained in cosmic rays and in some experiments at the LHC evident in favor of a new state of matter existence. If this idea is correct, it can be investigated at LHC in detail. But it is necessary to search for the new state of matter at LHC not in proton-proton interactions but in nucleus-nucleus interactions. It is better to do this in interactions of light nuclei (nitrogen, oxygen), for which the multiplicity of secondary particles is not so large compared to Pb-Pb or Au-Au.

This work was performed with the financial support of the Ministry of Education and Science of the Russian Federation (government task and MEPhI Academic Excellence Project). Authors thank R.P. Kokoulin for fruitful discussions which appreciably improved this paper.

References

1. K. Nakamura et al. (Particle Data Group), J. Phys. G **37**, 075021 (2010).
2. A. Petrukhin, Measurements of EAS muon energy – the key to solution of primary cosmic ray energy spectrum problem, in Proc. 31st Int. Cosmic Ray Conf., 2009, Lodz, Poland (http://icrc2009.uni.lodz.pl/proc/pdf/icrc0884.pdf).
3. G.V. Kulikov, G.B. Khristiansen, Soviet Physics JETP **35**, 441 (1959).
4. J. Blumer, R. Engel, J.R. Horandel, Progress in Particle and Nuclear Physics **63**, 293 (2009).
5. S.A. Slavatinski, Nucl. Phys. B (Proc.Suppl.) **122**, 3 (2003).
6. M. Tamada, Nucl. Phys. B (Proc.Suppl.) **122**, 349 (2003).
7. V.I. Yakovlev, Nucl. Phys. B (Proc.Suppl.) **122**, 417 (2003).
8. S.I. Nikolsky, Nuclear Physics B (Proc. Suppl.) **60B**, 144 (1998).
9. Yu.V. Stenkin, Phys. of Atomic Nuclei **71**, 98 (2008).
10. I.M. Dremin, EPJ Web of Conferences **145**, 10003 (2017).
11. M. Tamada, N. Inoue, A. Misaki, A. Ohsawa, EPJ Web of Conferences **145**, 15001 (2017)
12. S.B. Shaulov, P.F. Beyl, R.U. Beysembaev et al., EPJ Web of Conferences **145**, 17001 (2017).
13. V. Avati, L. Dick, K. Eggert, J. Strom, H. Wachsmuth, S. Schmeling, T. Ziegler, A. Bruhl, C. Grupen, Astropart. Phys. **19**, 513 (2003).
14. J. Abdallah et al. (DELPHI Collab.), Astroparticle Physics **28**, 273 (2007).
15. A.G. Bogdanov, D.M. Gromushkin, R.P. Kokoulin, G. Mannocchi, A.A. Petrukhin, O. Saavedra, G. Trinchero, D.V. Chernov, V.V. Shutenko, I.I. Yashin, Phys. of Atomic Nuclei **73**, 1852 (2010).
16. A. Aab et al. (Pierre Auger Collaboration), Phys. Rev. D **91**, 032003 (2015).
17. P. Sokolsky, Nucl. Phys. B (Proc. Suppl.) **212-213**, 74 (2011).
18. A. Aab et al. (Pierre Auger Collaboration), Phys. Rev. D **90**, 122005 (2014).

19. A.G. Bogdanov, R.P. Kokoulin, Yu.F. Novoseltsev, R.V. Novoseltseva, V.B. Petkov, A.A. Petrukhin, Astropart. Phys. **36**, 224 (2012).
20. A.A. Petrukhin, Nucl. Instrum. Meth. A **742**, 228 (2014).
21. T.K. Nayak, Pramana **79**, 719 (2012).
22. A. Toia, CERN Courier **53** (N 4), 31 (2013).
23. Z.-T. Liang, X.-N. Wang, Phys. Rev. Lett. **94**, 102301 (2005).
24. J.-H. Gao, S.-W. Chen, W.-T. Deng, Z.-T. Liang, Q. Wang, X.-N. Wang, Phys. Rev. C **77**, 044902 (2008).
25. A. Petrukhin, Nucl. Phys. B (Proc. Suppl.) **212-213**, 235 (2011).
26. A.A. Petrukhin, V.I. Galkin, M.G. Kogan, R.P. Kokoulin, S.Yu. Matveev, V.S. Puchkov, Nucl. Phys. B (Proc. Suppl.) **196**, 165 (2009).
27. A. Petrukhin, Nucl. Phys. B (Proc. Suppl.) **175-176**, 125 (2008).
28. A. Petrukhin, Nuovo Cimento B **120**, 837 (2005).
29. G. Aad et al. (ATLAS Collaboration), Phys. Rev. Lett. **105**, 252303 (2010).
30. K. Aamodt et al. (ALICE Collaboration) Phys. Rev. Lett. **105**, 252301 (2010).